Polymer Testing 90 (2020) 106598

Contents lists available at ScienceDirect

Polymer Testing

journal homepage: http://www.elsevier.com/locate/polytest

Effect of blend composition and related morphology on the quasi-static fracture performance of LLDPE/PP blends

Caren Rosales [a], Celina Bernal [b], Valeria Pettarin [a,*]

[a] Polymer Science and Engineering Group, Institute of Materials Science and Technology (INTEMA), University of Mar Del Plata - CONICET, Av. Colon 10850, 7600, Mar Del Plata, Argentina

[b] Polymers and Composites Engineering Group, Institute of Technology in Polymers and Nanotechnology, (ITPN), University of Buenos Aires - CONICET, Av. Las Heras 2214, 1127, Buenos Aires, Argentina

ARTICLE INFO

Keywords:
Polyethylene
Polypropylene
Polymer blends
Fracture behavior
Morphology

ABSTRACT

In the present work, the effect of composition and related morphology on the fracture behavior of LLDPE/PP blends was thoroughly investigated. Fracture behaviors evaluated under quasi-static loading conditions and different fracture mechanics methodologies were applied to assess fracture toughness depending on the materials behavior. For pure PP and 2575 blend, *J* at instability was chosen whereas for blends which exhibited completely ductile behavior (such as LLDPE, 7525 and 5050), the EWF methodology was used. Fracture mechanisms were elucidated with the aid of scanning electron microscopy, and results correlated with blends morphology. It was observed that fracture properties are mostly dominated by the majority component properties. In addition, for the 5050 blend, the presence of a co-continuous morphology is responsible for the high scatter of experimental data obtained.

1. Introduction

Characterization of polymer blends has been of great interest in recent decades since blending is an easy and efficient strategy to generate new polymeric materials with improved performance. In part, this is due to the interest in designing new materials that include or share the advantages of its pure components. On the other side, there are cases in which blending is unavoidable [1]. The latter situation is the case of polyethylene (PE) and polypropylene (PP) from post-consumer waste. Both polyolefins have very similar characteristics that make them difficult and expensive to separate with the usual industrial strategies (for example, flotation). Then, the need to solve an environmental problem requires reprocessing polyethylene and polypropylene as mixtures [2–4].

It is known that blend properties are strongly dependent on the microstructure and phase morphology of the constituent materials, and their interaction. Several studies have been conducted about blends between different types of polyethylene (lineal, low density, high density) and varying relative amount of PP [5]. Furthermore, this kind of blends have been compatibilized with various copolymers [6–10] and processed by all plastics conventional processing methods. Mourad et al. [11] made a good summary of the current bibliography, specifying the idea of each one. An exhaustive work of the scientific community has been carried out to understand how blending influences morphology, thermal and rheological properties [12–18], and especially, mechanical behavior of these blends.

However, investigation related to the mechanical properties always empathized in conventional mechanical characterization, i.e., tensile and impact tests (Izod or Charpy) [5,7,12,14–16,19], but these tests are not always sensitive to microstructural differences and related parameters are not useful for design purposes. Meanwhile, even though fracture toughness is an essential design parameter, it has not been studied in depth for many polymers and blends. It is indicative of the material resistance to fracture in the presence of a sharp crack, which is not completely avoidable in the processing of a polymeric material. The resistance to fracture in a blend is affected by several factors:

- the compatibility between constituents;
- the presence and amount of compatibilizer, which determines the particle size of the minority phase in the blend and interfacial interactions between phases;
- the intrinsic characteristics of the material of the matrix [20].

However, the determination of fracture parameters is not a trivial

* Corresponding author.
E-mail address: pettarin@fi.mdp.edu.ar (V. Pettarin).

https://doi.org/10.1016/j.polymertesting.2020.106598
Received 21 December 2019; Received in revised form 29 April 2020; Accepted 30 April 2020
Available online 4 June 2020
0142-9418/© 2020 Elsevier Ltd. All rights reserved.

task, much less for a blend. That is the reason why no studies regarding the fracture behavior and deformation mechanisms of PE/PP systems have been reported at the time of writing, to the authors' knowledge.

This work is the natural sequel of a previous work, in which morphology and tensile performance of LLDPE/PP blends was reported [21]. The novelty of the present work relies in the study of the influence of blending in the fracture performance of LLDPE/PP blends, in the entire range of compositions. To the best of authors' knowledge, there is no such a report in the literature. The fracture resistance of LLDPE/PP blends was studied in detail. Blends were evaluated under quasi-static loading conditions. The effect of blending content on the resistance to crack initiation, subsequent crack propagation, and energy consumed or dissipated during the fracture process, and fracture toughness were quantified by different fracture mechanics methodologies, depending on the materials behavior. Failure modes and micromechanical and toughening mechanisms were elucidated with the aid of scanning electron microscopy on post-mortem specimens, and results were correlated with blends morphology.

2. Experimental

2.1. Materials and blends preparation

Polyolefin blends were prepared based on commercial linear low density polyethylene (LLDPE) Dowlex IP20 (MI = 20 gr/10 min (190 °C/2.16 kg)) from Dow Argentina, and polypropylene (PP) 1100SC (MI = 25 gr/10 min (230 °C/2.16 kg)) from Cuyolen Petroquímica Cuyo, Argentina. As compatibilizer a block copolymer was added, 2630 PC (MI = 20 gr/10 min (190 °C/2.16 kg)) from Cuyolen. Studied materials (blends and homopolymers) are detailed in Table 1.

PP and PE pellets were manually premixed in a container and then mixed in a twin screw extruder, with temperatures from hooper to die equal to 150, 170 and 200 °C, at a rotational speed of 80 rpm. Plaques of 60 mm width, 100 mm length and 2 mm thick of all materials were obtained by injection molding, using a Multiplast 10T molding machine equipped with a double gated injection mold. Processing parameters were previously optimized [21] and were set as: injection temperature = 210 °C; injection speed = 45 mm/s; injection pressure = 22 MPa; injection time = 3 s; packing pressure = 21 MPa; packing time = 15 s; cooling time = 20 s; mold temperature = 20 °C.

Functional groups and chemical bonds analysis of blends were performed by means of FTIR analysis. A Nicolet 6700 FTIR-spectrometer was used, using a Attenuated Total Reflection (ATR) attachment. Each spectra were recorded with a resolution of 4 cm^{-1} and consisted of 64 scans from 500 to 4000 cm^{-1} at 23°C. Two replicas from each sample were used to obtain each spectra.

2.2. Microstructure and fracture surface morphology analysis

Microstructure was characterized in a previous work by SEM observations of cryogenically fractured specimens [21]. In order to complete fracture characterization, the surface morphology of fractured deeply double edge notched tensile (DDENT) specimens was also studied. Micrographs were taken with a Jeol JSM 6460 scanning electron microscope (SEM), after they had been coated with a thin layer of gold.

Table 1
Composition and nomenclature of the samples analyzed.

Sample	PE (wt%)	PP (wt%)	Copolymer (wt%)
PE	100	0	0
7525	72.5	22.5	5
5050	47.5	47.5	5
2575	22.5	75.2	5
PP	0	100	0

2.3. Fracture characterization

Rectangular specimens of nominal width W of 25 mm and nominal length S of 50 mm were obtained from injected plates. In order to evaluate inhomogeneities induced by/during processing, samples were cut from different sites of injected parts: flow direction (FD) and transverse flow direction (TFD), loaded parallel and perpendicular to the melt flow direction, respectively. As the plaques contain a welding line due to the double gated injection used, specimens including welding line (WL) were also cut. Sharp notches were introduced by sliding a scalpel (13 μm in radius) with a Ceast Notchvis notching machine. Samples are schematized in Fig. 1. Exploratory fracture tests were carried out using DDENT under quasi-static loading conditions. Tests were performed at room temperature with a crosshead speed of 2 mm/min on a universal testing machine Instron 4467. To evaluate results confidence, 5 replications were performed for each piece position for all blends with notch length to width ratio, a/W = 0.5.

To identify fracture behavior several factors were evaluated: the fracture surface appearance, the load-displacement curve shape, and the concept of ductility level (DL). DL was introduced by Martinez et al. [22], and for DDENT specimens, DL is defined as the ratio of displacement at rupture and initial ligament length (l). Then, fracture behavior is classified according to DL value as brittle fracture ($DL < 0.1$), ductile instability ($0.1 < DL < 0.15$), post yielding ($0.15 < DL < 1$), blunting ($1 < DL < 1.5$) and necking ($D < 1.5$). Different fracture mechanics approaches – J-integral at instability point and essential work of fracture – were applied to evaluate materials toughness, according to the observed fracture behavior.

2.3.1. J-integral at instability point

The value of the J-integral at initiation, J_{Ic}, is shown to be a good measure of toughness in cases where there is no significant crack growth resistance [23,24].

The J-integral is conventionally defined for nonlinear elastic materials as a path independent line integral. The multi-specimen procedure offers a more conservative approach to obtain a JR curve because each data point comes from a separate specimen. Nevertheless, the J formulation for single-specimen has been extensively used in the past to characterize ductile fracture in polymers [25]. Although ASTM E813 and ASTM E1152 standards apply only to ductile fracture, more recent standards, allow the application of J-integral to test materials that fail by cleavage. The J_c parameter [26] can be applied to characterize materials that exhibit load–displacement curves with sharp load drop at the point

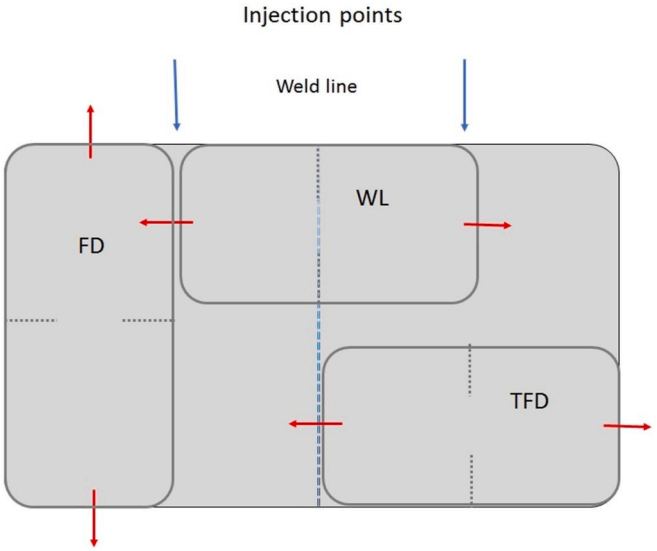

Fig. 1. Scheme of the location of specimens extracted from the injected plates.

of fracture, i.e. quasi-brittle failure behavior, by using specimens with a crack to depth ratio close to 0.5. J_c was evaluated at the instability load point by calculating the fracture energy required to produce cleavage behavior of pre-cracked specimens having a crack depth-to-width ratio of $0.45 < a/W < 0.55$ as:

$$J_c = \frac{\eta\, U_{tot}}{B(W-a)} \tag{1}$$

where U_{tot} is the instability fracture energy, i.e., the area under the load–deflection curve till the instability point, B is the thickness of tested specimens, and η is a geometry factor that for DDENT specimens is expressed as [27]:

$$\eta = -0.06 + 5.99\left(\frac{a}{W}\right) - 7.42\left(\frac{a}{W}\right)^2 + 3.29\left(\frac{a}{W}\right)^3 \tag{2}$$

The *J*-integral approach is a natural extension of linear elastic fracture mechanics and works best for not too ductile fractures.

2.3.2. Essential work of fracture

According to the Essential Work of Fracture (EWF) theory, the total work required to fracture a notched specimen can be divided in two parts associated with two zones [28]. The first part is related to a process zone where the actual crack is running. The energy associated with it, the essential work of fracture, (W_e) is proportional to the ligament section lt. The second part is related to a plastic zone, which surrounds the process zone and the energy involved there is the non-essential work of fracture or plastic work (W_p), which is proportional to the volume of the deformed region. It can be written therefore:

$$W_f = W_e + W_p = w_e.lt + \beta w_p.l^2 t \tag{3}$$

where w_e is the specific essential work of fracture (per unit ligament area), w_p is the specific non-essential work of fracture (per unit volume), l is the ligament length, t is the specimen thickness and β is the plastic zone shape factor. Dividing eq (3) by the ligament area lt, the specific work of fracture is obtained, w_f:

$$w_f = W_f/_{lt} = w_e + \beta w_p \tag{4}$$

An important prerequisite of the plane stress EWF approach is that crack propagates only after the ligament has been fully yielded, and load-displacement curves should be self-similar among all specimens tested while ligament length is varying.

3. Results

3.1. Blends morphology and chemical characterization

In order to correlate fracture results with morphology, SEM images of cryogenic fracture surfaces are presented here. Morphology of blends is a critical parameter which affects mechanical performance, i.e. size and distribution are very important when toughening process is studied [29,30]. Micrographs of neat polymers and blends are shown in Fig. 2. Morphology varies from the typical particulate morphology of minority phase for the 2575 and 7525 blends to a co-continuous like phase for the 5050 blend, characteristic of immiscible blends. The size of second phase particles was very small and finely dispersed into the matrix. This morphology is related with processing parameters, volume fraction and different properties of polymer components, such as viscosity ratio, interfacial adhesion, etc (see Ref. [21]). As PP has a limited compatibility with LLDPE, small voids (see yellow arrows in Fig. 2-a and c) are observed on the cryo-fractured surface because of the pullout of LLDPE droplets from the matrix [31]. This is due the absence of strong interactions between the two polymer components [29,32]. More details are given in a previous work [21], and are similar to other authors findings [5,9,33,34]. Regarding the morphology near the weld line, elongated particles are present probably due to the elongation stresses induced by flow during mold filling. A clear example of this situation is shown in Fig. 2-c and 2-d in which the same blend is shown but in different location in the injected plaque, far from welding line and in welding line, respectively.

ATR-FTIR analysis was performed on pure LLDPE, PP and their

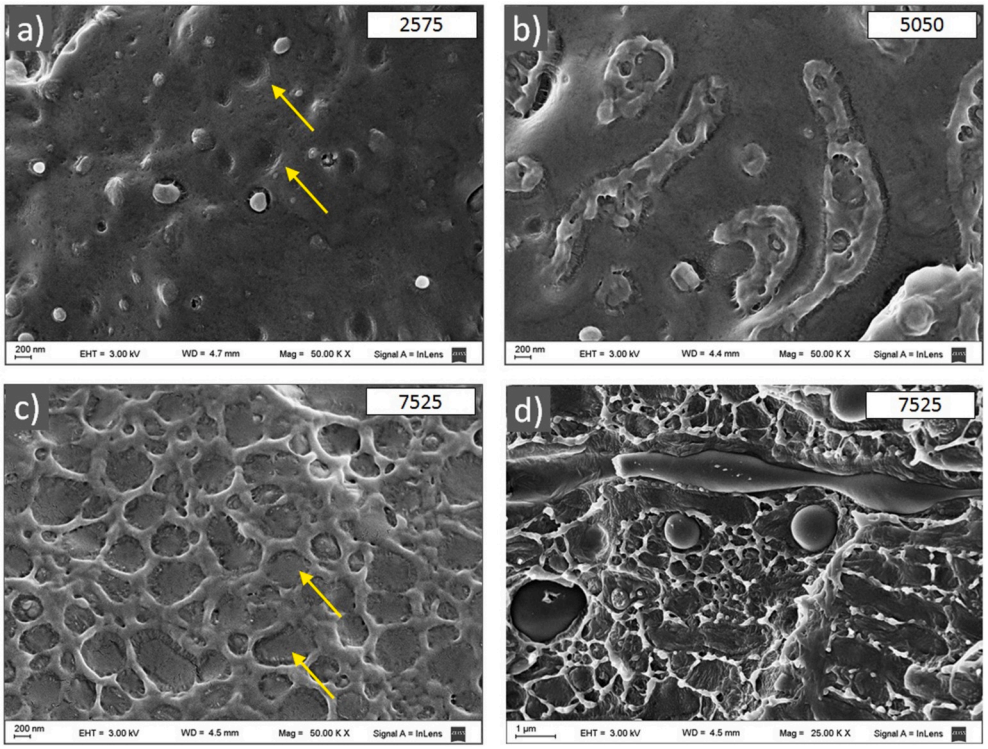

Fig. 2. SEM micrographs from cryo-fractured surfaces: a) DF 7525, b) DF 5050, c) DF 2575 and d) WL 7525.

blends in order to connect IR ray's due to energy absorbed by blends with the corresponding vibrational energy of bonds of different functional groups [35]. ATR was used because of its inherent advantage of obtaining the spectra directly from the sheet, without any further sample preparation [36]. Obtained FTIR spectra are shown in Fig. 3 and assignment of absorption peaks of IR spectrum are listed in Table 2.

There are four and two peaks corresponding to pure PP and LLDPE respectively in the wavenumber range 3000–2800 cm^{-1}. The peaks at 2955 and 2873 cm^{-1} are attributed to CH_3 asymmetric and symmetric stretching vibrations respectively, and the peaks at 2922 and 2843 cm^{-1} are due to CH_2 asymmetric and symmetric stretching vibrations respectively, and are obviously present in both samples. Observing lower wave numbers, there are four additional peaks: at 1460 cm^{-1}, caused by CH_3 asymmetric deformation vibrations or CH_2 scissor vibrations; at 1368 cm^{-1}, due to CH_3 symmetric deformation vibrations; at 730 cm^{-1}, due to CH_2 rocking vibration of crystalline phase; and at 718 cm^{-1}, attributed to CH_2 rocking vibration of the amorphous phase [37–39].

In the spectra corresponding to the blends, the same two regions previously mentioned are clearly observed. PP or LLDPE characteristics are seen to be more pronounced with increasing PP or LLDPE relative content, indicating that the same functional groups are present, but in different proportions [35], and no changes in chemical structure is induced by blending. It has been pointed out in literature that when extensive compatibilization occurs between components of a blend, structural changes can be detected by FTIR [38,39]. As no structural changes are observed in our blends, it is concluded that there is no evidence of a good compatibilization between components.

Moreover, previously analysis by X-ray diffraction indicated that the characteristic crystals of PP and LLDPE are retained [21], namely, the intrinsic crystal structure of both PE and PP are not influenced by the presence of the other constituent, neither in the surface nor in the core of injected pieces.

3.2. Quasi-static tensile behavior

Tensile behavior was studied in a previous work [21], and the obtained results are summarized in what follows, to give an insight into conventional mechanical behavior of blends. It was observed that all blends exhibited typical ductile behavior under quasi-static tensile loading, with a maximum in the stress-strain curve related to the initiation of necking. Materials' tensile parameters are depicted in Table 3. They were found to be very dependent on the blend composition, increasing with increasing PP content, due to the higher stiffness and crystallinity of this polymer respect to LLDPE [5]. It was also observed

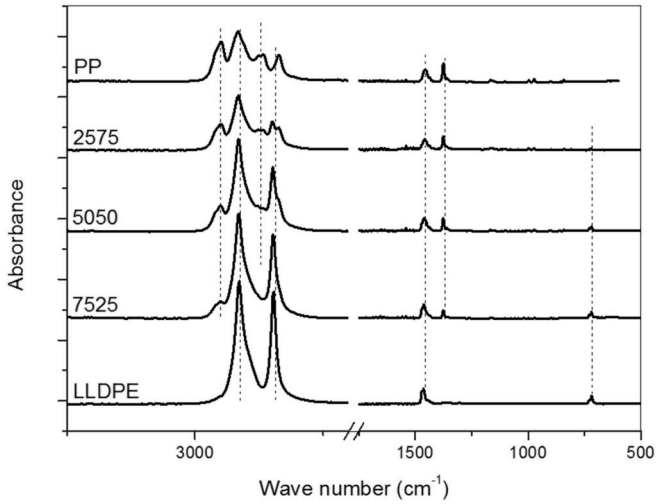

Fig. 3. ATR-FTIR spectra of pure PP, pure LLDPE and their blends.

Table 2
Assignment of functional groups to absorption peaks obtained in FTIR.

Wave number (cm^{-1})	Assigned groups	Present samples
2955	CH_3 (asymmetrical)	PP
2922	CH_2 asymmetric	PP, LLDPE
2873	CH_2 Stretching (symmetrical)	PP
2843	CH_2 symmetric stretching vibrations	PP, LLDPE
1460	CH_3 asymmetric deformation vibrations or CH_2 scissor vibrations	PP, LLDPE
1368	CH_3 symmetric deformation vibrations	PP
730	CH_2 Rocking vibration, crystalline	LLDPE
718	CH_2 Rocking vibration, amorphous	LLDPE

that yield strength and Young's Modulus values vary following the rule of mixtures [5,6,12]. The ductility of blends was lower than that of homopolymers, i.e. blends failed much more quickly than pure PP and LLDPE. The necking during stretching of a polymer is, in fact, an expression of the yield behavior of the material mainly attributable to the morphological structure and the nature of the interface between the two phases [22]. It was observed a negative deviation from a rule of mixtures typically due to the embrittlement common in incompatible plastic blends [34].

3.3. Fracture behavior

Typical load-displacement curves obtained in quasi-static fracture tests on DENT samples are shown in Fig. 4 together with macroscopic photographs of tested specimens in the flow direction (FD) for all materials. It is observed that the shape of load-displacement curves significantly varied as the relative amount of LLDPE increases: the fracture behavior changes from ductile instability to completely ductile (necking). At the same time, maximum load gradually decreases whereas the displacement at break increases.

A more detailed insight in fracture behavior in all evaluated locations of injected samples (DF, DTF and WL) is presented in Fig. 5, and corresponding fracture surfaces are shown in Fig. 6.

A semi-brittle behavior is observed for PP (Fig. 5-a), regardless of the load direction, with a typical smooth fracture surface with no sign of plastic deformation (Fig. 6-a and b).

2575 blend is in the ductile-brittle transition zone. Some 2575 blend samples failed in a ductile mode, and the other specimens – that do not exhibit fully ductile mode of failure – present two different behaviors: semi-brittle (for TFD and WL samples) and semi-ductile (for FD samples) (Fig. 5-b). The semi-ductile behavior can be easily explained by SEM observations of fracture surfaces (Fig. 6-a). Skin delamination and stretching are the cause of the apparent large deformations observed in ductile samples.

Samples of the 5050 blend show differences between locations in injected pieces. DF samples achieve larger maximum loads and elongation at break than TFD and WL samples (see dotted curves in Fig. 5-c). The slope of load-displacement curves during the tearing stage of fracture process is much steeper for TFD and WL samples than for DF ones, suggesting less stable crack propagation in the former blends, in which load is applied transversal to flow direction, i.e. perpendicular to

Table 3
Quasi-static tensile properties of blends.

Sample	Tensile parameters		
	Young modulus (MPa)	Yield strength (MPa)	Elongation at break (mm/mm)
LLDPE	387 ± 22	8,7 ± 0,5	5,4 ± 0,5
7525	609 ± 21	12,9 ± 0,3	0,8 ± 1,2
5050	933 ± 42	16,3 ± 1,1	0,4 ± 0,3
2575	1158 ± 121	24,9 ± 1,7	1,3 ± 1,7
PP	1367 ± 55	31,9 ± 1,9	3,4 ± 1,2

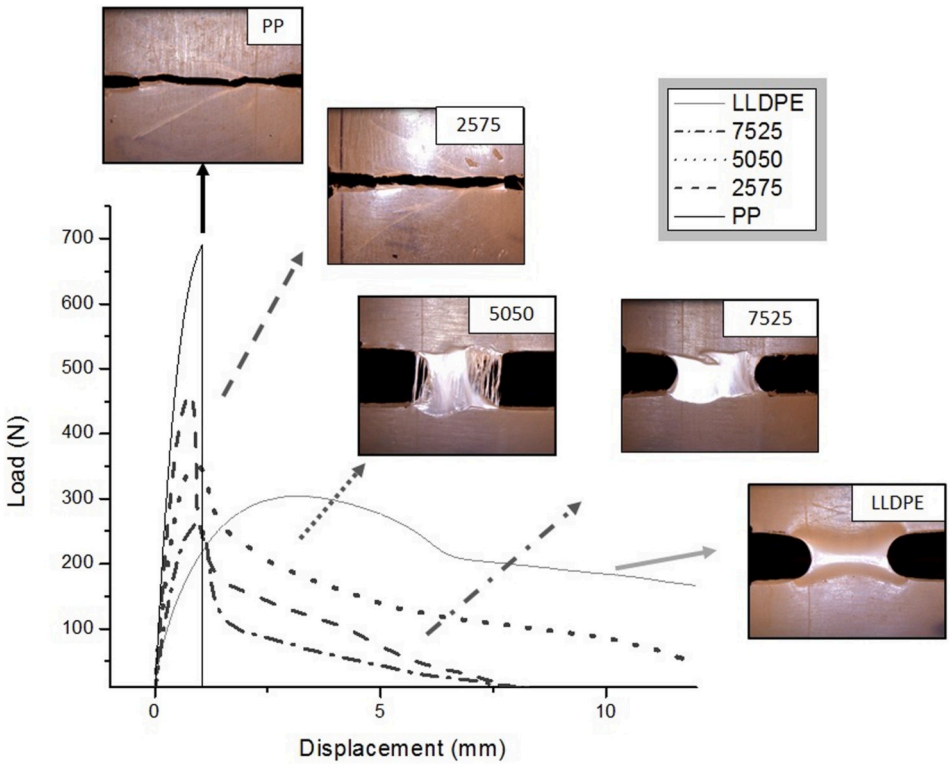

Fig. 4. Load-displacement curves and macroscopic damage images.

macromolecules orientation. Observation of the macro photographs demonstrated that the specimen damage development is initiated by crack blunting that grows until the maximum load, followed by necking and stable crack propagation. It is observed in SEM micrographs that the presence of PP domains causes matrix cavitation which triggers crazing and matrix fibrillation (Fig. 6-f).

7525 and LLDPE samples show a completely ductile behavior, with no apparent differences between locations in pieces, indicating that inhomogeneities induced by the process are not determining factors of the fracture behavior of these materials. Observations of the macro photographs indicate that failure mechanisms are similar to those of 5050 blend, i.e. crack blunting, necking and stable crack propagation. SEM observations for 7525 samples are similar to those for 5050 samples, but with longer and more homogeneously distributed fibrils in the fracture surface (Fig. 6-g).

3.4. Fracture mechanisms

The deformation mechanism for 2575 and 7525 blends is outlined in Fig. 7-a. Their micrographs reveals the formation of cavities which are related to the detachment of PP or LLDPE particles (depending on the blend composition) from the matrix on mechanical loading. This is due to the decohesion process of dispersed particles from surrounding matrix and development of voids at the interfaces. These findings denote poor interfacial adhesion between particles and matrix in LLDPE/PP blends (despite the presence of compatibilizer), which results in unavailing stress transfer from the matrix to domains during tension mechanical loading. However, particle cavitation has been largely discussed for rubber or elastomer modification as toughening mechanism [28,29]. Cavitation process is associated with the formation of fibre like structure inside the matrix. During loading, fracture energy given to the blend is absorbed by the matrix. This absorption leads to fibrils formation in the path of the fracture propagation and the pulling out of the dispersed phase from the matrix. Therefore the particles remain intact [20,40,41]. This mechanism seems to operate in our blends. Subsequently, no toughening effect can be achieved from this mechanism for LLDPE/PP blends. The fibrillation effect is more noticeable in the case of highest concentration of LLDPE. The number and appearance of the fibers change from 2575 to 7525 blend.

In the case of 5050 blend, the deformation mechanism differs from the one sketched above, and it is outlined in Fig. 7-b. In this co-continuous morphology, PP fails in a more brittle manner, while LLDPE presents a fibrillar deformation. Then, the macroscopic response and toughness depends on the notch path and the components it find in its path. This is the reason of the observed dispersion in both fracture behavior and toughness of 5050 blend.

It seems that a more fine and uniform distribution of PP particles as the one of 7525 samples [21] favors matrix cavitation and fibrillation. In the case of LLDPE, fibrillation is maximized, and very stretched fiber bunches are observed (Fig. 5-h and i). Crack initiation and growth in polyethylene is known to take place through formation and subsequent breakdown of a craze zone ahead of the crack tip [42,43]. Localized plastic strains, initiation and coalescence of voids, and formation of fibrils that eventually fail drive this process [44].

The above observations correlate well with *DL* calculations, which are shown in Fig. 8 as a function of blend composition (the effect of inhomogeneities is also included). *J*-Integral at maximum load was selected as the parameter to evaluate toughness of samples exhibiting ductile instability [22]. The essential work of fracture method is strictly applicable only to post-yielding fracture behavior, while for necking or blunting another requirements suggested by the ESIS TC-4 Committee must also be fulfilled. Taking into account these recommendations, the EWF methodology was applied for ductile samples (7525 and 5050 blends, and LLDPE). As the 2575 blend exhibited both ductile and brittle behavior, i.e. a ductile-fragile transition, the EWF method was not applicable, and *J* at maximum load was selected as the fracture toughness parameter in this case.

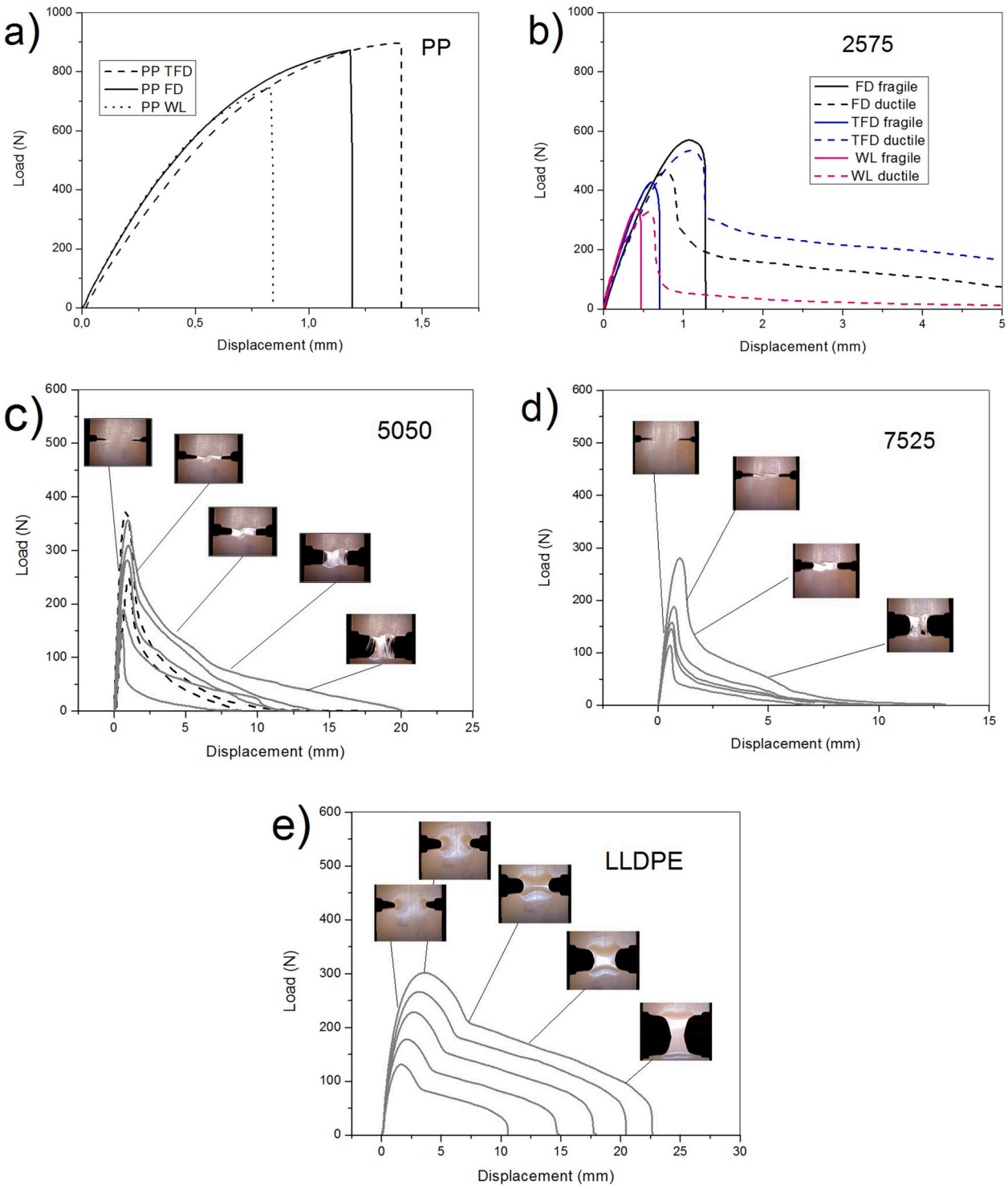

Fig. 5. Load-displacement curves for all blends: a) PP, b) 2575, c) 5050, d)7525 and e) LLDPE.

3.5. Jc determination

Based on previous observations, J_c was selected as the fracture mechanics approach to evaluate fracture toughness for PP and 2575 samples. In the case of PP, J_c at instability calculation is direct. However, for the 2575 blend, instability point was estimated as the area just after the maximum load drop point, due to the large differences observed in energy for being in the ductile-brittle range.

Obtained J_c values for both materials are shown in Table 4. J_c values are similar for FD and TFD samples, with a lower value in the case of WL samples, as expected due to the weakness of the welded zone [45–47]. This effect is emphasized in 2575 samples due to the complex morphology developed during molding, i.e. elongated second phase domains parallel to weld line (see Fig. 2-d) that act as sharp stress concentrators.

3.6. EWF analysis

As it can be observed in Fig. 5-c, d and e, in which load-displacement curves for different ligament lengths for LLDPE, 7525 and 5050 blends

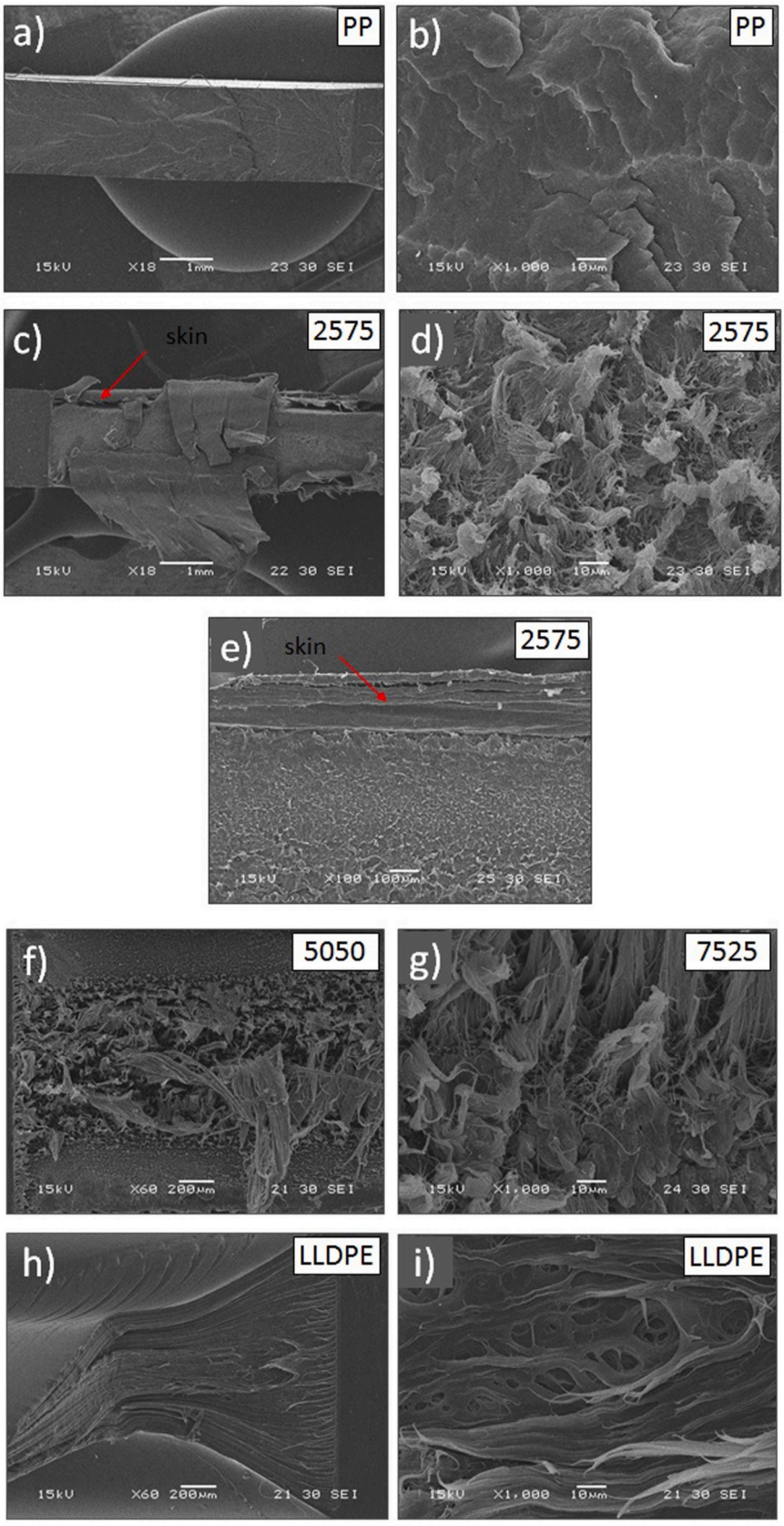

Fig. 6. SEM micrographs obtained from fracture surfaces of all materials at different magnification.: a) PP specimen, b) PP fracture surface, c) 2575 skin delamination, d) 2575 fibrillation, e) 2575 skin induced by processing, f) 5050 bulk fibrillation, g) 7525 longer fibrillation, h) LLDPE massive plastic deformation and, i) LLDPE extensive fibrillation.

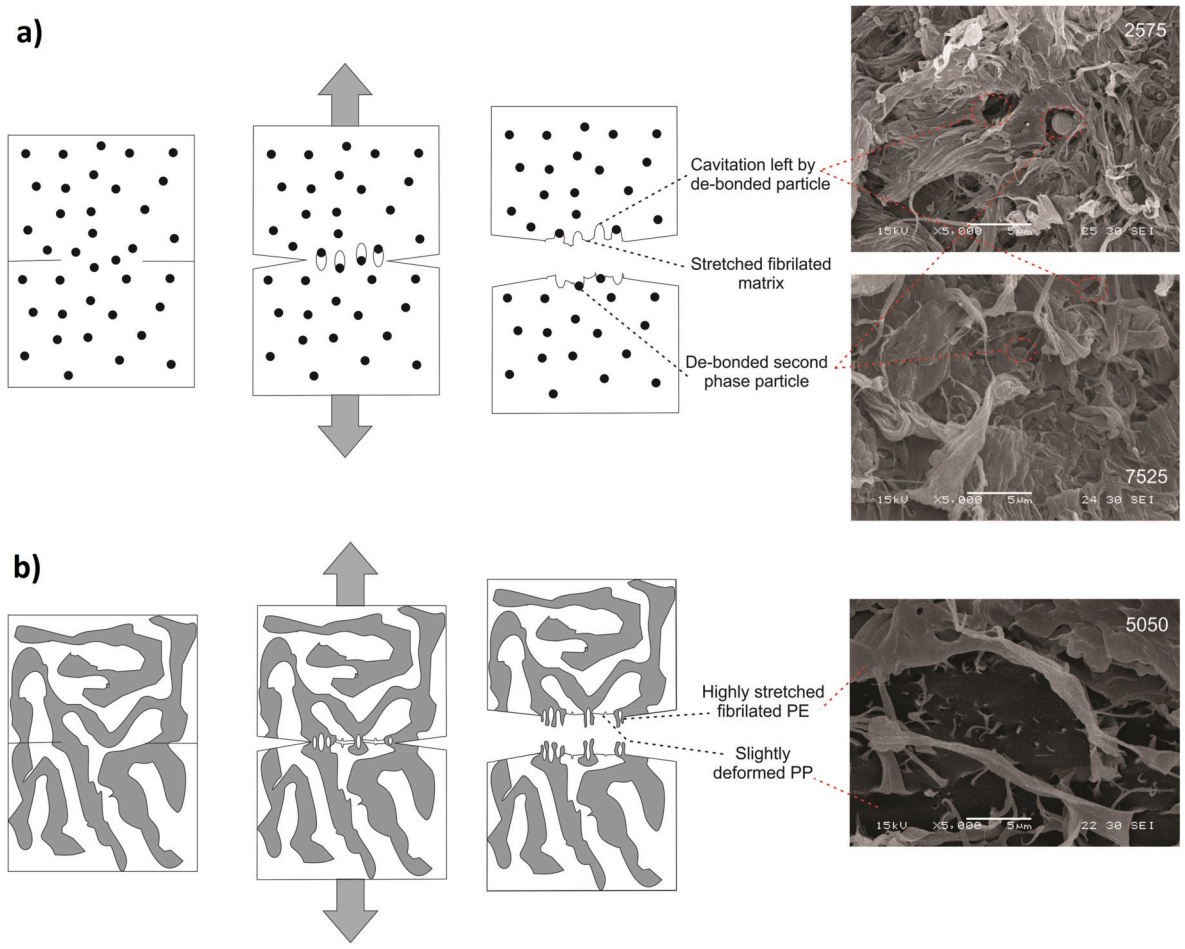

Fig. 7. Scheme of the deformation and failure mechanisms proposed for (a) 7525 and 2575 blends; (b) 5050 blend.

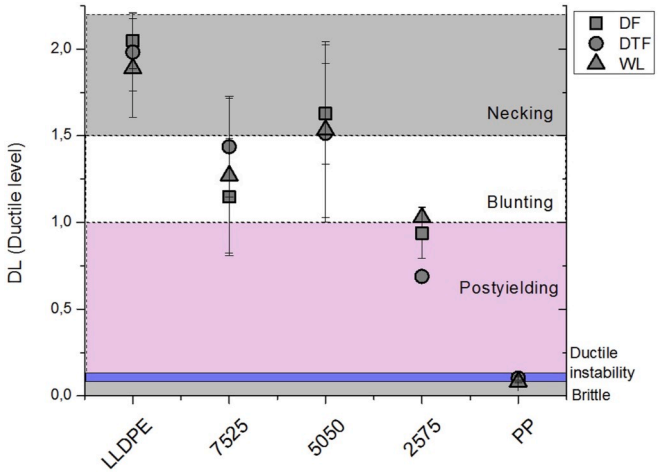

Fig. 8. Ductility level depending on the pure constituents, blend composition and solicitation direction.

are shown, the ligament yields before crack propagation, validating the applicability of the EWF method [48]. In the case of the 5050 blend, load-displacement curves similarity requirement is not completely fulfilled. This self-similarity pre-requisite ensures that crack propagation occurs under similar stress conditions, in spite of the different ligament lengths. It is a first indication that the w_e parameter cannot be extracted in the traditional way in this case [49].

Table 4
J_c values for pure PP and 2575 blend.

Sample	Position	J_c (KJ/m^2)
PP	FD	35.9 ± 5.0
	TFD	33.3 ± 5.7
	WL	26.2 ± 3.3
2575	FD	18.0 ± 2.7
	TFD	13.5 ± 2.0
	WL	8.5 ± 4.3

EWF determination by linear fitting regression of specific work of fracture *vs* ligament is shown in Fig. 9, for LLDPE, and 7525 and 5050 blends, for FD samples as an example. Dispersion data are within the acceptable range for LLDPE [50] and the 7525 blend, but not for the 5050 blend, as expected.

However, displacement curves for 5050 samples showed self-similarity until load drop just after the maximum load (Fig. 5-c). For this type of curves, an approach that suggests an energy partition between yielding and necking for EWF tests has been proposed in the literature [51]. The procedure is schematized in Fig. 10. This partition is applicable for load-displacement curves that have a characteristic behavior where the yielding is separated from the subsequent necking by a drop of load. This point is easily identified in the curve and means a clear transition between the beginning and the propagation of cracks. The first part corresponds to the work required for yielding (until the load fall) while the second part is related to the work required for necking (equation (5)). In this way, the value $w_{e,y}$ represents the inherent initiation parameter of the material. This approach has been

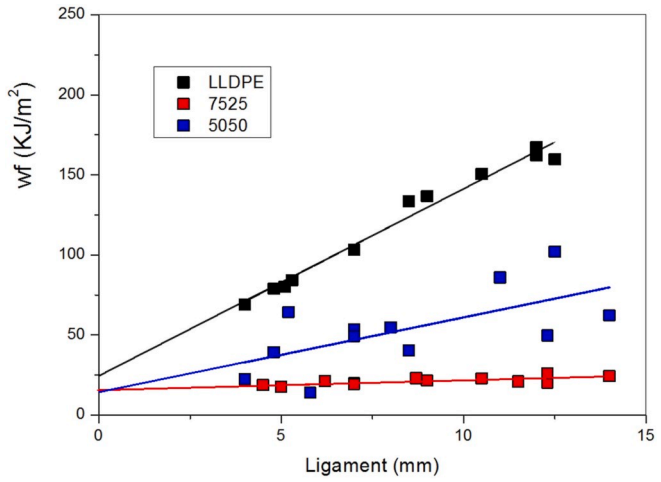

Fig. 9. Comparison of the w_f vs l curves for LLDPE, and the 7525 and 5050 blends, for FD samples.

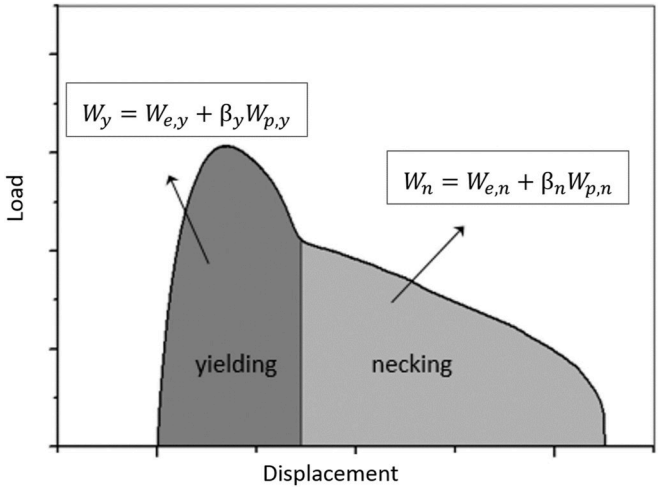

Fig. 10. Schematic representation of the energy partitioning between yielding and necking.

applied by several authors [48,52,53].

$$w_f = w_y + w_n = (w_{e,y} + \beta_y w_{p,y} l) + (w_{e,n} + \beta_n w_{p,n} l) \quad (5)$$

where $w_{e,y}$ and $w_{e,n}$ are the specific essential work for yielding and necking, respectively. Furthermore, $w_{p,y}$ and $w_{p,n}$ are non-essential work of yielding and necking, respectively. The values β_y and β_n are geometry factors associated with the shape of the plastic zone during yielding and necking, respectively.

Then, based on the shape of the curves of LLDPE, and the 7525 and 5050 blends; and on the poor linear adjustment observed for the 5050 blend, we decided to split the curves into two zones, i.e. to split the specific work of fracture. To ensure that EWF tests were performed under plane stress conditions, ESIS TC4 protocol suggests a criterion on the maximum stress values ($\sigma_{max} = P_{max}/_{lt}$) for DDENT specimens, as proposed by Clutton [54]. According to this protocol, maximum stress values should be between 0.9 σ_m and 1.1 σ_m – being σ_m the average maximum stress - so that the plane-stress condition prevails. Then, in a plot of σ_{max} *versus* ligament length, the data lying outside these limits should be eliminated. An example of this procedure is shown in Fig. 11 for FD LLDPE samples. Fig. 12 shows the new fitting curves of yielding specific work of fracture *vs.* ligament (including points not took into account due to plane stress criterion). The parameters of essential and non-essential yielding work of fracture for LLDPE, and the 7525 and 5050 blends, were calculated by extrapolating the linear fit of w_f *vs.* l points in corresponding range of σ_m to zero ligament length, and are shown in Table 5.

When comparing different materials at the same location, the initiation parameter $w_{e,y}$ is similar for the 7525 and 5050 blends, and smaller than the value for LLDPE. These binary blends between LLDPE and PP have a high degree of incompatibility and low interfacial adhesion [21] so, there is low load transfer between phases and the particles act as stress concentrators, promoting defects creation and a path for crack propagation [48]. Addition of 25% PP had an impact not only on the essential work of fracture but also on the non-essential work of fracture. It can be seen that LLDPE presents a greater plastic work, while the 7525 blend samples fail with a minimum plastic zone formation, considering that the term βw_f is close to zero. In LLDPE samples chains defolding and stretching occur before the rupture and crack propagation, producing a large plastic zone [51]. On the other side, in the 7525 blend, the second phase (or minority phase) works as an internal restriction on the matrix polymer, which restricts its capacity for mass deformation and, therefore, the formation of a larger plastic zone. It is noticeable that the 5050 blend exhibits a higher propagation value. This mixture presents a co-continuous like structure, and it is known that the formation of these structures can impart polymer blends with a good stiffness-toughness balance [55,56]. It was stated that large propagation values are observed when failure is not confined to the fracture plane and extend to the bulk [57]. This may be happened in the 5050 blend, due to the co-continuous structure that is able to transfer the load to larger volumes. Moreover, great dispersion in total energy could be attributed to the non-reproducibility of this mechanism in all samples.

When location in the sample is varied, all materials (LLDPE and the 7525 and 5050 blends) show a resistance to initiation (w_e) in flow direction (FD) greater than in transverse flow direction (TFD). This anisotropy could be explained by the formation of a crystalline structure oriented by the flow forces during mold filling, which results in toughness increase when the load direction coincides with the orientation direction. Applying a tension perpendicular to the direction of orientation results in a lower toughness value [57].

3.7. Influence of composition in fracture toughness

In order to compare fracture toughness of different blends, w_e values obtained from evaluation of complete curves (before partitioning) and J_c values are plotted in Fig. 13. It is easily observed that fracture toughness values for all blends are lower than the values for each of the constituents, even lower than the value obtained from a rule of mixtures. This is

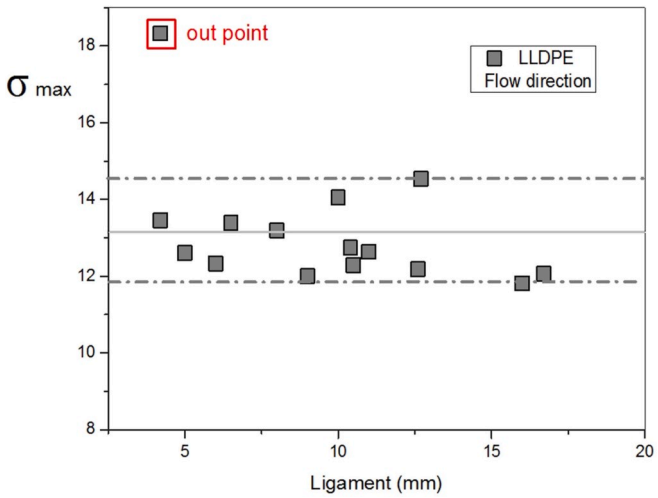

Fig. 11. σ_{max} values vs. ligament length for LLDPE in flow direction.

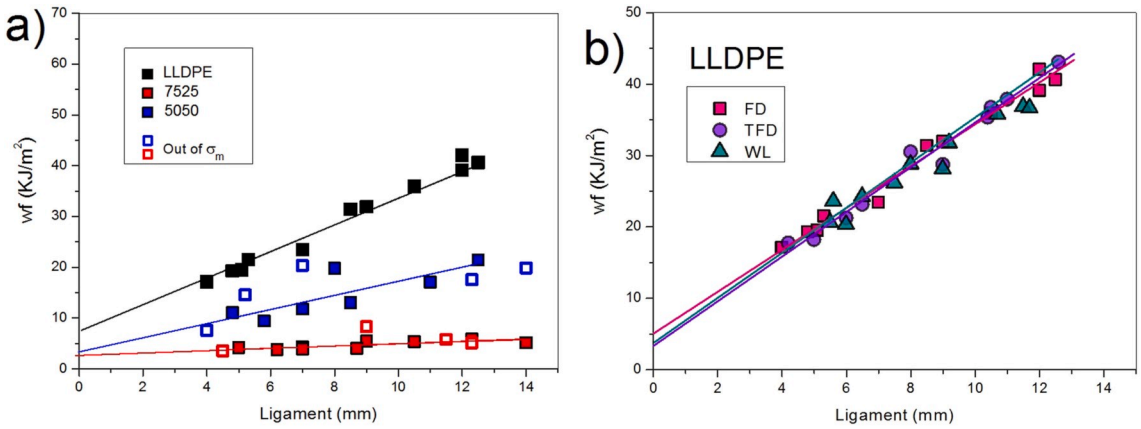

Fig. 12. Typical work of fracture *versus* ligament length plots comparing (a) different materials (b) different sample locations for the same material.

Table 5
EWF parameters for LLDPE, the 7525 and 5050 blends.

Sample	Position	w_e (KJ/m^2)	βw_f (MJ/m^3)
LLDPE	FD	5.2 ± 1.0	2.9 ± 0.1
	TFD	3.3 ± 1.4	3.1 ± 0.2
	WL	5.0 ± 1.7	2.6 ± 0.2
7525	FD	2.9 ± 0.6	0.2 ± 0.1
	TFD	1.4 ± 0.5	0.3 ± 0.1
	WL	0.7 ± 1.2	0.2 ± 0.1
5050	FD	3.3 ± 1.7	1.4 ± 0.4
	TFD	1.5 ± 1.2	0.7 ± 0.1
	WL	–	–

mainly due to the high incompatibility between LLDPE and PP. The J_c parameter represents the resistance to unstable crack propagation, and the addition of 25% of LLDPE to PP turns this value 50% lower than for pure PP. A similar observation can be done for w_e parameter, i.e. 5050 and 7525 blends present a lower value than that one of pure LLDPE. The weak interfacial adhesion is responsible for creating several stress concentrators that easily create a crack path.

In order to obtain a competitive blend in terms of fracture behavior, another strategy such as the incorporation of an elastomeric phase [58–61] and/or morphology manipulation [62–64] should be intended.

4. Conclusions

In the present work, the effect of the composition and the related morphology on the fracture behavior of LLDPE/PP blends was thoroughly investigated.

Different fracture mechanics approaches were used to characterize the materials fracture performance depending on their fracture behavior. For pure PP and 2575 blend, J at instability was chosen, whereas for ductile behavior the EWF methodology was used (For LLDPE, 7525 and 5050). From the results of this investigation, it can be concluded that fracture properties are mostly dominated by the majority component properties. For the 5050 blend, the presence of a co-continuous morphology is responsible for the high scatter of experimental data obtained.

Currently, further strategies such as the incorporation of an elastomeric phase and/or morphology manipulation are being carried out to achieve useful and cheap materials from post-consumer wastes, comparable to virgin polyolefins.

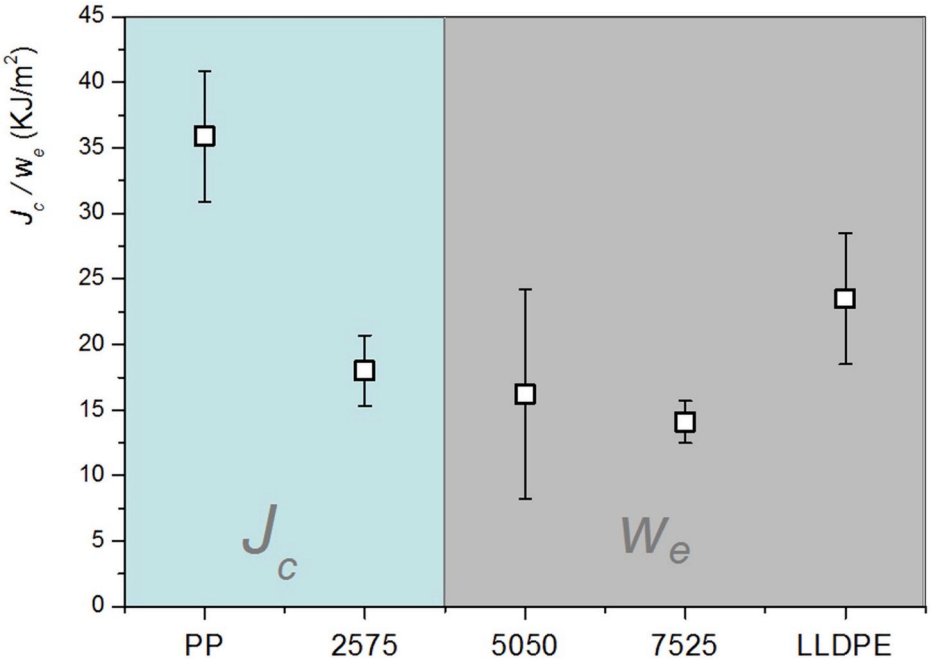

Fig. 13. Fracture toughness vs. composition.

5. Data availability

The raw/processed data required to reproduce these findings cannot be shared at this time as the data also forms part of an ongoing study.

Declaration of competing interest

The authors declare that they have no known competing financial interests or personal relationships that could have appeared to influence the work reported in this paper.

CRediT authorship contribution statement

Caren Rosales: Data curation, Formal analysis, Investigation, Writing - original draft. **Celina Bernal:** Conceptualization, Formal analysis, Funding acquisition, Methodology, Supervision, Writing - review & editing. **Valeria Pettarin:** Conceptualization, Formal analysis, Funding acquisition, Methodology, Project administration, Supervision, Writing - review & editing.

Acknowledgements

Authors would like to thank University of Mar del Plata (UNMdP) and University of Buenos Aires (UBA) for financial support.

Appendix A. Supplementary data

Supplementary data to this article can be found online at https://doi.org/10.1016/j.polymertesting.2020.106598.

References

[1] B. Na, R. Lv, Z. Zhao, Dispersed microfibril-dominated deformation and fracture behaviors of linear low density polyethylene/isotactic polypropylene blends, J. Appl. Polym. Sci. 104 (2007) 1291–1298, https://doi.org/10.1002/app.

[2] S. Bertin, J. Robin, Study and characterization of virgin and recycled LDPE/PP blends, Eur. Polym. J. 38 (2002) 2255–2264.

[3] C. Fang, L. Nie, S. Liu, R. Yu, N. An, S. Li, Characterization of polypropylene-polyethylene blends made of waste materials with compatibilizer and nano-filler, Compos. B Eng. 55 (2013) 498–505, https://doi.org/10.1016/j.compositesb.2013.06.046.

[4] I. Borovanska, T. Dobreva, R. Benavente, S. Djoumaliisky, G. Kotzev, Quality assessment of recycled and modified LDPE/PP blends, Elastomers Plast (2012) 1–19, https://doi.org/10.1177/0095244312441731.

[5] N.V. Penava, V. Rek, I.F. Houra, Effect of EPDM as a compatibilizer on mechanical properties and morphology of PP/LDPE blends, J. Elastomers Plastics 45 (2013) 391–403, https://doi.org/10.1177/0095244312457162.

[6] G. Radonjič, N. Gubeljak, The use of ethylene/propylene copolymers as compatibilizers for recycled polyolefin blends, Macromol. Mater. Eng. 287 (2002) 122–132, https://doi.org/10.1002/1439-2054(20020201)287:2<122::AID-MAME122>3.0.CO;2-A.

[7] C. Clemons, Elastomer modified polypropylene-polyethylene blends as matrices for wood flour-plastic composites, Compos. Part A Appl. Sci. Manuf. 41 (2010) 1559–1569, https://doi.org/10.1016/j.compositesa.2010.07.002.

[8] M. Yang, K. Wang, L. Ye, Y.-W. Mai, J. Wu, Low density polyethylene-polypropylene blends: Part 1 - ductility and tensile properties, Plast. Rubber Compos. 32 (2003) 21–26, https://doi.org/10.1179/146580103225009112.

[9] J.W. Teh, A. Rudin, J.C. Keung, A review of polyethylene–polypropylene blends and their compatibilization, Adv. Polym. Technol. 13 (1994) 1–23, https://doi.org/10.1002/adv.1994.060130101.

[10] C. Tselios, D. Bikiaris, V. Maslis, C. Panayiotou, In situ compatibilization of polypropylene–polyethylene blends: a thermomechanical and spectroscopic study, Polymer 39 (1998) 6807–6817, https://doi.org/10.1016/S0032-3861(98)00132-3.

[11] A.H.I. Mourad, Thermo-mechanical characteristics of thermally aged polyethylene/polypropylene blends, Mater. Des. 31 (2009) 918–929, https://doi.org/10.1016/j.matdes.2009.07.031.

[12] S. Jose, A.S. Aprem, B. Francis, M.C. Chandy, P. Werner, V. Alstaedt, S. Thomas, Phase morphology , crystallisation behaviour and mechanical properties of isotactic polypropylene/high density polyethylene blends, Eur. Polym. J. 40 (2004) 2105–2115, https://doi.org/10.1016/j.eurpolymj.2004.02.026.

[13] A.C.Y. Wong, Heat deflection characteristics of polypropylene and polypropylene/polyethylene binary systems, Compos. B Eng. 34 (2003) 199–208, https://doi.org/10.1016/S1359-8368(02)00080-X.

[14] R.A. Shanks, J. Li, L. Yu, Polypropylene-polyethylene blend morphology controlled by time-temperature-miscibility, Polymer 41 (2000) 2133–2139, https://doi.org/10.1016/S0032-3861(99)00399-7.

[15] A. Dhoble, B. Kulshreshtha, S. Ramaswami, D.A. Zumbrunnen, Mechanical properties of PP-LDPE blends with novel morphologies produced with a continuous chaotic advection blender, Polymer 46 (2005) 2244–2256, https://doi.org/10.1016/j.polymer.2005.01.057.

[16] G. Shan, W. Yang, B. Xie, M. Yang, Mechanical properties and morphology of LDPE/PP blends, J. Macromol. Sci. 46 (2007) 963–974, https://doi.org/10.1080/00222340701457253.

[17] M. Jin, R. La, Y. Zhang, K. Liu, X. Li, J. Zhang, Stratiform b crystals in ultrahigh molecular weight polyethylene and b -nucleating agent-nucleated isotactic polypropylene at micro-injection molding condition, Polym. Test. 42 (2015) 135–143.

[18] T. Wu, Y. Li, G. Wu, Crystalline structure and phase structure of mLLDPE/LDPE blends, Polymer 46 (2005) 3472–3480, https://doi.org/10.1016/j.polymer.2005.02.084.

[19] R. Strapasson, S.C. Amico, M.F.R. Pereira, T.H.D. Sydenstricker, Tensile and impact behavior of polypropylene/low density polyethylene blends, Polym. Test. 24 (2005) 468–473, https://doi.org/10.1016/j.polymertesting.2005.01.001.

[20] D. xiang Sun, C. jin Yang, X. dong Qi, J. hui Yang, Y. Wang, Largely enhanced fracture toughness of the PP/EPDM blends induced by adding carbon nanofibers, Compos. Sci. Technol. 164 (2018) 146–152, https://doi.org/10.1016/j.compscitech.2018.05.048.

[21] C. Rosales, D. Brendstrup, C. Bernal, V. Pettarin, Morphology/tensile performance relationship for LLDPE/PP double gated injected blends, Adv. Mater. Lett. 11 (2) (2019) 1–6.

[22] A.B. Martinez, J.I. Velasco, O.O. Santana, M.L. Maspoch, The essential work of fracture (EWF) method – analyzing the post-yielding fracture mechanics of polymers, Eng. Fail. Anal. 16 (2009) 2604–2617, https://doi.org/10.1016/j.engfailanal.2009.04.027.

[23] E. Plati, J.G. Williams, The determination of the fracture parameters for polymers in impact, Polym. Eng. Sci. 15 (1975) 470–477, https://doi.org/10.1002/pen.760150611.

[24] A. Stocchi, V. Pettarin, A. Izer, T. Bárány, T. Czigány, C. Bernal, Fracture behavior of recyclable all-polypropylene composites composed of α- and β-modifications, J. Thermoplast. Compos. Mater. 24 (2011) 805–818, https://doi.org/10.1177/0892705711401850.

[25] A.R. Shahani, H. Shooshtar, M. Baghaee, On the determination of the critical J-integral in rubber-like materials by the single specimen test method, Eng. Fract. Mech. 184 (2017) 101–120, https://doi.org/10.1016/j.engfracmech.2017.08.031.

[26] Astm E1820, Standard Test Method for Measurement of Fracture Toughness, ASTM, Philadelphia, n.d, 1996.

[27] W. Grellmann, K. Reincke, Quality improvement of elastomers – application of instrumented notched tensile-impact testing for assessment of toughness, Mater. Prufung. 46 (2004) 168–175.

[28] R.J. Cotterell B, The essential work of plane stress ductile fracture 13 (1977) 267–277.

[29] C. Harrats, S. Thomas, G. Groeninckx, Micro- and Nanostructured Multiphase Polymer Blend Systems, 2006.

[30] R.J. Gaymans, W.C.J. Zuiderduin, D.P.N. Vlasveld, J. Hue, Mechanical properties of polyketone terpolymer/rubber blends, 45, 2004, https://doi.org/10.1016/j.polymer.2004.03.080, 3765–3779.

[31] M. Yang, K. Wang, L. Ye, Y.-W. Mai, J. Wu, Low density polyethylene-polypropylene blends: Part 2 - strengthening and toughening with copolymer, Plast. Rubber Compos. 32 (2003) 27–31, https://doi.org/10.1179/146580103225009095.

[32] A.R. Ajitha, S. Thomas, Introduction, Elsevier Inc., 2020, https://doi.org/10.1016/b978-0-12-816006-0.00001-3.

[33] A. Luciani, J. Jarrin, Morphology development in immiscible polymer blends, Polym. Eng. Sci. 36 (1996) 1619–1626, https://doi.org/10.1002/9781118892756.ch19.

[34] A.M. Kunjappan, A.A. Ramachandran, M. Padmanabhan, L.P. Mathew, S. Thomas, Selective localization of MWCNT in poly (trimethylene terephthalate)/poly ethylene Blends : theoretical analysis , morphology , and mechanical properties, Macromol. Symp. 381 (2018) 1–6, https://doi.org/10.1002/masy.201800104.

[35] J. Petrovich, FTIR and DSC of polymer films used for packaging: LLDPE, PP and PVDC, Shape Am. High Sch. (2015) 1–13. http://homepages.rpi.edu/~ryuc/outreach_1/2015_004_John_P.pdf.

[36] J.V. Gulmine, P.R. Janissek, H.M. Heise, L. Akcelrud, Polyethylene characterization by FTIR, Polym. Test. 21 (2002) 557–563, https://doi.org/10.1016/S0142-9418(01)00124-6.

[37] S.M. Al-Salem, M.H. Behbehani, A. Al-Hazza'a, J.C. Arnold, S.M. Alston, A.A. Al-Rowaih, F. Asiri, S.F. Al-Rowaih, H. Karam, Study of the degradation profile for virgin linear low-density polyethylene (LLDPE) and polyolefin (PO) plastic waste blends, J. Mater. Cycles Waste Manag. 21 (2019) 1106–1122, https://doi.org/10.1007/s10163-019-00868-8.

[38] R. Morent, N. De Geyter, C. Leys, L. Gengembre, E. Payen, Comparison between XPS- and FTIR-Analysis of Plasma-Treated Polypropylene Film Surfaces, 2008, pp. 597–600, https://doi.org/10.1002/sia.2619.

[39] W. Wu, Y. Wang, Physical and thermal properties of high-density polyethylene film modified with polypropylene and linear low-density polyethylene, J. Macromol. Sci. Part B Phys. 59 (2020) 213–222, https://doi.org/10.1080/00222348.2019.1709710.

[40] A. Reghunadhan, J. Datta, N. Kalarikkal, J.T. Haponiuk, S. Thomas, Toughness augmentation by fibrillation and yielding in nanostructured blends with recycled

polyurethane as a modifier, Appl. Surf. Sci. 442 (2018) 403–411, https://doi.org/10.1016/j.apsusc.2018.02.128.
[41] M.M. Mazidi, R. Berahman, A. Edalat, Phase morphology, fracture toughness and failure mechanisms in super-toughened PLA/PB-g-SAN/PMMA ternary blends: a quantitative analysis of crack resistance, Polym. Test. 67 (2018) 380–391, https://doi.org/10.1016/j.polymertesting.2018.03.028.
[42] H.R. Brown, A molecular interpretation of the toughness of glassy polymers, Macromolecules 24 (1991) 2752–2756. http://cat.inist.fr/?aModele=afficheN&cpsidt=19751685. accessed February 20, 2017.
[43] D.M. Duan, J.G. Williams, Craze testing for tough polyethylene, J. Mater. Sci. 33 (1998) 625–638, https://doi.org/10.1023/A:1004369107748.
[44] M. Kroon, E. Andreasson, V. Petersson, P.A.T. Olsson, Experimental and numerical assessment of the work of fracture in injection-moulded low-density polyethylene, Eng. Fract. Mech. 192 (2018) 1–11, https://doi.org/10.1016/j.engfracmech.2018.02.004.
[45] M.A. Costantino, V. Pettarin, A.J. Pontes, P.M. Frontini, Mechanical performance of double gated injected metallic looking polypropylene parts, Express Polym. Lett. 9 (2015) 1040–1051, https://doi.org/10.3144/expresspolymlett.2015.93.
[46] C. Lu, S. Guo, L. Wen, J. Wang, Weld line morphology and strength of polystyrene/polyamide-6/poly(styrene- co-maleic anhydride) blends, Eur. Polym. J. 40 (2004) 2565–2572, https://doi.org/10.1016/j.eurpolymj.2004.06.016.
[47] J.C. Viana, A.J. Pontes, U. Nacional, D. Mar, A. Costantino, V. Pettarin, Morphology-performance relationship of PP- nanoclay composites processed by shear controlled injection moulding Morphology – performance relationship of polypropylene – nanoclay composites processed by shear controlled injection, Polym. Int. 62 (2013) 1589–1599, https://doi.org/10.1002/pi.4543.
[48] M. Haghnegahdar, G. Naderi, M.H.R. Ghoreishy, Fracture toughness and deformation mechanism of un-vulcanized and dynamically vulcanized polypropylene/ethylene propylene diene monomer/graphene nanocomposites, Compos. Sci. Technol. 141 (2017) 83–98, https://doi.org/10.1016/j.compscitech.2017.01.015.
[49] J. Karger-Kocsis, D.E. Mouzakis, Effects of injection molding-induced morphology on the work of fracture parameters in rubber-toughened polypropylenes, Polym. Eng. Sci. 39 (1999) 1365–1374.
[50] F.M. Peres, J.R. Tarpani, C.G. Schön, Essential work of fracture testing method applied to medium density polyethylene, Procedia Mater. Sci. 3 (2014) 756–763, https://doi.org/10.1016/j.mspro.2014.06.124.
[51] D.E. Mouzakis, J. Karger-Kocsis, Essential work of fracture: application for polymers showing ductile-to-brittle transition during fracture, Polym. Bull. 42 (1999) 473–480, https://doi.org/10.1007/s002890050491.
[52] M.L. Maspoch, A.B. Martinez, O.O. Santana, On the essential work of fracture method : energy partitioning of the fracture process in iPP films, Polym. Bull. 42 (1999) 101–108.
[53] M. Mehrabi Mazidi, M.K. Razavi Aghjeh, Synergistic toughening effects of dispersed components in PP/PA6/EPDM ternary blends; Quantitative analysis of the fracture toughness via the essential work of fracture (EWF) methodology, RSC Adv. 5 (2015) 47183–47198, https://doi.org/10.1039/c5ra07193c.
[54] E.Q. Clutton, ESIS TC4 experience with the essential work of fracture method, Eur. Struct. Integr. Soc. 27 (2000) 187–199.
[55] L.A. Utracki, Commercial Polymer Blends, Chapman & Hall, London, 1998, p. 98.
[56] P. Potschke, D.R. Paul, Blends, Macromol. Sci. Part C. Polym. Rev. 43 (2003) 87–141.
[57] J. Karger-Kocsis, Microstructural and molecular dependence of the work of fracture parameters in semicrystalline and amorphous polymer systems, Eur. Struct. Integr. Soc. 27 (2000) 213–230, https://doi.org/10.1016/S1566-1369(00)80020-5.
[58] F.D.B. de Sousa, J.R. Gouveia, P.M.F. de Camargo Filho, S.E. Vidotti, C. H. Scuracchio, L. Amurin, T.S. Valera, Blends ground tire rubber devulcanized by microwaves/HDPE - Part B: influence of clay addition, Polim. E Tecnol. 25 (2015) 382–391, https://doi.org/10.1590/0104-1428.1747.
[59] C.R. Kumar, I. Fuhrmann, J. Karger-Kocsis, LDPE-based thermoplastic elastomers containing ground tire rubber with and without dynamic curing, Polym. Degrad. Stabil. 76 (2002) 137–144, https://doi.org/10.1016/S0141-3910(02)00007-1.
[60] J. Karger-kocsis, Use of ground tyre rubber (GTR) in thermoplastic polyolefin elastomer compositions, Prog. Rubber Plast. Recycl. Technol. 20 (2004).
[61] O. Grigoryeva, a. Fainleib, O. Starostenko, I. Danilenko, N. Kozak, G. Dudarenko, Ground tire rubber (GTR) reclamation: virgin rubber/reclaimed GTR (RE) vulcanizates, Rubber Chem. Technol. 77 (2004) 131–146, https://doi.org/10.5254/1.3547806.
[62] M.E. Wenjing Li, Alois K. Schlarb, Influence of processing window and weight ratio on the morphology of the extruded and drawn PET/PP blends, Acta Med. Okayama 70 (2016) 111–118, https://doi.org/10.1002/pen.
[63] M. Kuzmanović, L. Delva, D. Mi, C.I. Martins, L. Cardon, K. Ragaert, Development of Crystalline Morphology and its Relationship with Mechanical Properties of PP/PET Microfibrillar Composites Containing POE and POE-G-MA, 2018, https://doi.org/10.3390/polym10030291. Polymers (Basel).
[64] D. Višnjić, H. Lalić, V. Dembitz, H. Banfić, Extrusion of polyethylene/polypropylene blends with microfibrillar-phase morphology, Martina 116 (2014) 37–43, https://doi.org/10.1002/pc.